

Impurity states in graphene with intrinsic spin-orbit interaction

M Ingot¹ ‡ and V K Dugaev^{1,2}

¹ Department of Physics, Rzeszów University of Technology, Al. Powstańców
Warszawy 6, 35-959 Rzeszów, Poland

² Department of Physics and CFIF, Instituto Superior Técnico, Technical University
of Lisbon, Av. Rovisco Pais, 1049-001 Lisbon, Portugal

E-mail: ming@prz.edu.pl

Abstract. We consider the problem of electron energy states related to strongly localized potential of a single impurity in graphene. Our model simulates the effect of impurity atom substituting the atom of carbon, on the energy spectrum of electrons near the Dirac point. We take into account the internal spin-orbit interaction, which can modify the structure of electron bands at very small neighborhood of the Dirac point, leading to the energy gap. This makes possible the occurrence of additional impurity states in the vicinity of the gap.

PACS numbers: 73.22Pr, 73.20Hb

1. Introduction

Graphene attracted a lot of attention recently due to very unusual properties of electron energy spectrum and transport properties, including both the transport of electrons and phonons [1, 2, 3, 4, 5]. The most striking properties of graphene are related to the energy spectrum near the Dirac points, where this spectrum is linear as a function of momentum, and the Hamiltonian of free electrons can be described by the relativistic two-dimensional Dirac model [6].

Naturally, the impurities and defects can strongly affect the energy spectrum of graphene. Especially important is the effect of impurities on the spectrum near the Dirac point. The impurity states and the corresponding variation of the electron density of states have been already discussed in several papers [7, 8, 9, 10] without taking into account the spin-orbit (SO) interaction. It was found that the localized impurity potential gives the resonant states in the spectrum of graphene. They can be located near the Dirac point in the case of relatively strong impurity potential, and this is quite unusual for the semiconductor physics. In the case of carbon vacancy, there appears a local energy level at the Dirac point, with $E = 0$. In all of these works, the main attention has been paid to a finite density of impurities and defects leading to modification of the density of states in graphene.

In this paper we mostly concentrate on the problem of single impurity taking into account the internal SO interaction. The SO interaction opens a gap in the electron energy spectrum [11]. However, it was found that the magnitude of SO-induced gap is very small in graphene [12, 13, 14, 15], and therefore it would be very difficult to observe this gap experimentally. Nevertheless, the problem exists: how this small gap would affect the behavior of impurity states in the vicinity of Dirac point?

We demonstrate that the SO gap induces appearance of additional impurity states corresponding to very weak impurity potential. As a result, the SO gap in graphene can be experimentally unobservable due to a large number of adsorbed light atoms at the graphene surface creating the impurity states in the gap.

2. Model

We use the following Hamiltonian, which describes electrons near the Dirac point K , with the intrinsic SO interaction [11]

$$\hat{H}_{\mathbf{k}} = \begin{pmatrix} \sigma_z \Delta & vk_- \\ vk_+ & -\sigma_z \Delta \end{pmatrix}, \quad (1)$$

where Δ is the band splitting related to the SO interaction, v is the velocity parameter, and we denote $k_{\pm} = k_x \pm ik_y$. The matrix form of (1) is due to the choice of wavefunction basis corresponding to different sublattices in the lattice of graphene. The basis functions of Hamiltonian (1) are

$$|\mathbf{k}(1, 2)\sigma\rangle = \sum_{s \in (A, B)} e^{i(\mathbf{k}_0 + \mathbf{k}) \cdot \mathbf{r}_i} \psi_s(\mathbf{r}) |\sigma\rangle, \quad (2)$$

where $\psi_s(\mathbf{r})$ is the tight-binding electron state at site s belonging to sublattice A or B, \mathbf{k}_0 is the wave vector corresponding to the chosen Dirac point, and $\sigma = \uparrow, \downarrow$ refers to spin up and down states, respectively. The eigenvalues of Hamiltonian (1) are $E_{k1,2} = \pm\varepsilon_k$, where $\varepsilon_k = (\Delta^2 + v^2k^2)^{1/2}$, so that the value of $2|\Delta|$ is the energy gap. The Hamiltonian for the other Dirac point K' differs from (1) by the opposite sign in the diagonal terms. Thus, the results for the point K' can be found by using calculations with the Hamiltonian (1) and reverting the sign of Δ .

Since the SO interaction in Equation (1) does not mix the spins, one can consider separately spin up and down channels. For the spin up electrons the Hamiltonian can be presented as it gives the Hamiltonian for up-spin electrons

$$\hat{H}_{\mathbf{k}\uparrow} = \tau_z \Delta + v\boldsymbol{\tau} \cdot \mathbf{k}, \quad (3)$$

where τ_i are the Pauli matrices acting in the space of sublattices A and B. For the down-spin Hamiltonian, the sign of Δ in Equation (3) is opposite. We consider first the spin up Hamiltonian (3).

3. Nonmagnetic impurity

Let us consider the impurity state in the case of a single impurity, described by the perturbation localized in one of the sublattices. In the continuous model under consideration it corresponds to the perturbation at $\mathbf{r} = 0$ in sublattice A

$$\hat{V}_{\uparrow}(\mathbf{r}) = \begin{pmatrix} V_0 \delta(\mathbf{r}) & 0 \\ 0 & 0 \end{pmatrix}. \quad (4)$$

The matrix of perturbation (4) in the basis functions of Hamiltonian $\hat{H}_{\mathbf{k}\uparrow}$ is

$$\hat{V}_{\mathbf{k}\mathbf{k}'\uparrow} = \begin{pmatrix} V_0 & 0 \\ 0 & 0 \end{pmatrix} \equiv \hat{V}_{0\uparrow}. \quad (5)$$

The effect of perturbation $\hat{V}_{\mathbf{k}\mathbf{k}'\uparrow}$ on the energy spectrum in all orders of magnitude can be described using the T -matrix method [16]. In the general case, the equation for the T -matrix is

$$\hat{T}_{\mathbf{k}\mathbf{k}'}(\varepsilon) = \hat{V}_{\mathbf{k}\mathbf{k}'} + \sum_{\mathbf{k}_1} \hat{V}_{\mathbf{k}\mathbf{k}_1} \hat{G}_{\mathbf{k}_1}(\varepsilon) \hat{T}_{\mathbf{k}_1\mathbf{k}'}(\varepsilon), \quad (6)$$

where $\hat{G}_{\mathbf{k}}(\varepsilon) = (\varepsilon - \hat{H}_{\mathbf{k}})^{-1}$ is the Green's function of Hamiltonian $\hat{H}_{\mathbf{k}}$. Using (3) we find the Green's function for spin up electrons

$$\hat{G}_{\mathbf{k}\uparrow}(\varepsilon) = \frac{\varepsilon + \tau_z \Delta + v\boldsymbol{\tau} \cdot \mathbf{k}}{\varepsilon^2 - \varepsilon_k^2}. \quad (7)$$

In the following we assume that the energy parameter includes a small imaginary part, $\varepsilon \rightarrow \varepsilon + i\delta \operatorname{sgn} \varepsilon$, which corresponds to the choice of retarded Green's function. Using (5) and (7) we find

$$\hat{T}_{\uparrow}(\varepsilon) = \left[1 - \hat{V}_{0\uparrow} \sum_{\mathbf{k}} \hat{G}_{\mathbf{k}\uparrow}(\varepsilon) \right]^{-1} \hat{V}_{0\uparrow} \equiv \left[\hat{1} - \hat{V}_{0\uparrow} \hat{F}_{\uparrow}(\varepsilon) \right]^{-1} \hat{V}_{0\uparrow}, \quad (8)$$

and we have to calculate

$$\begin{aligned}\hat{F}_\uparrow(\varepsilon) &\equiv \sum_{\mathbf{k}} \hat{G}_{\mathbf{k}\uparrow}(\varepsilon) = -\frac{\varepsilon + \tau_z \Delta}{4\pi v^2} \ln \frac{v^2 k_m^2 + \Delta^2 - \varepsilon^2}{\Delta^2 - \varepsilon^2} \\ &\simeq -\frac{\varepsilon + i\delta \operatorname{sgn} \varepsilon + \tau_z \Delta}{4\pi v^2} \ln \frac{v^2 k_m^2 + \Delta^2 - \varepsilon^2 - 2i|\varepsilon|\delta}{\Delta^2 - \varepsilon^2 - 2i|\varepsilon|\delta},\end{aligned}\quad (9)$$

where the upper limit (cutoff) of integration over momentum k_m is introduced. It corresponds to the region of linearity of the spectrum near the Dirac point. Assuming $v^2 k_m^2 \gg |\Delta^2 - \varepsilon^2|$ we obtain

$$\hat{F}_\uparrow(\varepsilon) \simeq -\frac{\varepsilon + i\delta \operatorname{sgn} \varepsilon + \tau_z \Delta}{4\pi v^2} \left[\ln \frac{v^2 k_m^2}{[(\Delta^2 - \varepsilon^2)^2 + 4\varepsilon^2 \delta^2]^{1/2}} + i(\varphi_1 - \varphi_2) \right] \quad (10)$$

where $\varphi_{1,2}$ are the angles related to the phase of complex function $\hat{F}(\varepsilon)$, which can be made analytical in the whole complex plane of ε after proper choice of cuts in this plane. We assume that the cut is made along the real axis from $-|\Delta|$ to $+|\Delta|$. Then the phases can be chosen

$$\varphi_1 = -\tan^{-1} \frac{2|\varepsilon|\delta}{v^2 k_m^2}, \quad (11)$$

$$\varphi_2 = \begin{cases} \pi + \tan^{-1} \frac{2|\varepsilon|\delta}{|\varepsilon^2 - \Delta^2|}, & \varepsilon^2 > \Delta^2, \\ -\tan^{-1} \frac{2|\varepsilon|\delta}{|\varepsilon^2 - \Delta^2|}, & \varepsilon^2 < \Delta^2. \end{cases} \quad (12)$$

The real part of Equation (9)

$$\operatorname{Re} \hat{F}_\uparrow(\varepsilon) \simeq -\frac{\varepsilon + \tau_z \Delta}{4\pi v^2} \ln \frac{v^2 k_m^2}{[(\Delta^2 - \varepsilon^2)^2 + 4\varepsilon^2 \delta^2]^{1/2}}. \quad (13)$$

In the limit of $\delta \rightarrow 0$ (corresponding to small impurity density)

$$\operatorname{Re} \hat{F}_\uparrow(\varepsilon) \simeq -\frac{\varepsilon + \tau_z \Delta}{4\pi v^2} \ln \frac{v^2 k_m^2}{|\Delta^2 - \varepsilon^2|}, \quad (14)$$

$$\operatorname{Im} \hat{F}_\uparrow(\varepsilon) \simeq \begin{cases} \frac{\varepsilon + \tau_z \Delta}{4v^2}, & \varepsilon^2 > \Delta^2, \\ 0, & \varepsilon^2 < \Delta^2, \end{cases}. \quad (15)$$

The functions $\operatorname{Re} F_{11,\uparrow}(\varepsilon)$ and $\operatorname{Im} F_{11,\uparrow}(\varepsilon)$ are presented in figure 1 and figure 2.

The matrices $\hat{V}_{0\uparrow}$ and $\hat{F}_\uparrow(\varepsilon)$ are both diagonal. Therefore, $\hat{T}(\varepsilon)$ calculated from Equation (8) is diagonal, too

$$\hat{T}_\uparrow(\varepsilon) = \operatorname{diag} \left\{ \frac{V_{0\uparrow}}{1 - V_{0\uparrow} \operatorname{Re} F_{11,\uparrow}(\varepsilon) - iV_{0\uparrow} \operatorname{Im} F_{11,\uparrow}(\varepsilon)}, 0 \right\}. \quad (16)$$

The location of impurity level is determined by the pole of T -matrix

$$1 - V_{0\uparrow} \operatorname{Re} F_{11,\uparrow}(\varepsilon) = 0. \quad (17)$$

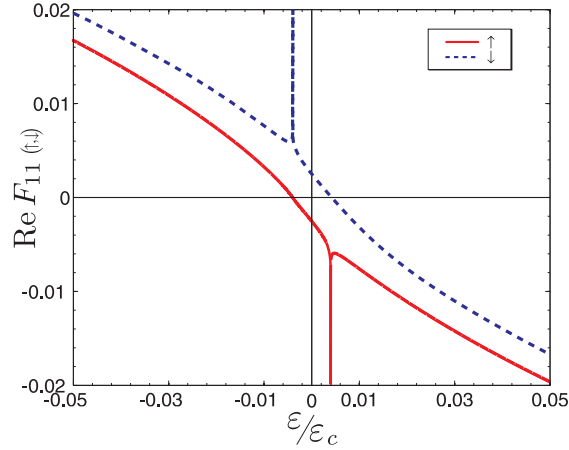


Figure 1. The dependence $\text{Re } F_{11}(\epsilon)$ for spin-up and spin down states, related to the Dirac point K in the case of non-magnetic impurity.

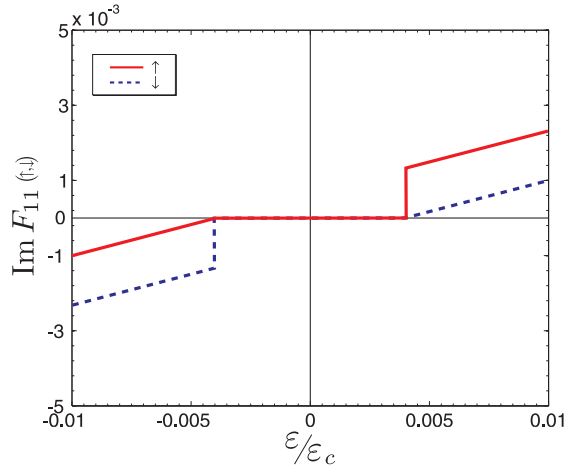


Figure 2. The imaginary part $\text{Im } F_{11}(\epsilon)$ for spin-up and spin down states, related to the point K in the case of non-magnetic impurity.

The dependence $\text{Re } F_{11,\uparrow}(\epsilon)$ presented in figure 1 can be used for the graphical solution of Equation (17). Using (14) we find

$$1 + V_{0\uparrow} \frac{\epsilon + \Delta}{4\pi v^2} \ln \frac{v^2 k_m^2}{|\Delta^2 - \epsilon^2|} = 0. \quad (18)$$

Thus, the equation for the impurity level is

$$\epsilon_{\uparrow} = -\Delta - \frac{4\pi v^2}{V_0 \ln \frac{v^2 k_m^2}{|\Delta^2 - \epsilon_{\uparrow}^2|}}. \quad (19)$$

This equation has several solutions for the same potential $V_{0\uparrow}$.

The Hamiltonian describing the spin down states

$$\hat{H}_{\mathbf{k}\downarrow} = -\tau_z \Delta + v \boldsymbol{\tau} \cdot \mathbf{k}, \quad (20)$$

differs from (2) only by the sign of gap parameter Δ . In the case of nonmagnetic impurity the perturbation $\hat{V}_\downarrow(\mathbf{r}) = \hat{V}_\uparrow(\mathbf{r})$. Performing the same calculations as before with the substitution $\Delta \rightarrow -\Delta$ we find the equation for impurity level corresponding to the spin-down state

$$\varepsilon_\downarrow = \Delta - \frac{4\pi v^2}{V_0 \ln \frac{v^2 k_m^2}{|\Delta^2 - \varepsilon_\downarrow^2|}}. \quad (21)$$

The spin up and down states corresponding to solution of Equation (19) and Equation (21), respectively, are split in energy. The magnitude of splitting is $2|\Delta|$, which of course is very small as was discussed in the Introduction. Nevertheless, considering the impurity states in the model with one Dirac point we come to a weakly magnetized state at the nonmagnetic impurity. This nonequivalence of spin up and down states is exactly compensated by the states related to another Dirac point, K' , for which the Hamiltonians of spin up and down states differ by the sign of Δ from those in Equation (3) and Equation (21) [11]. Thus, the magnetization of the localized state is absent if we take into account both nonequivalent Dirac points.

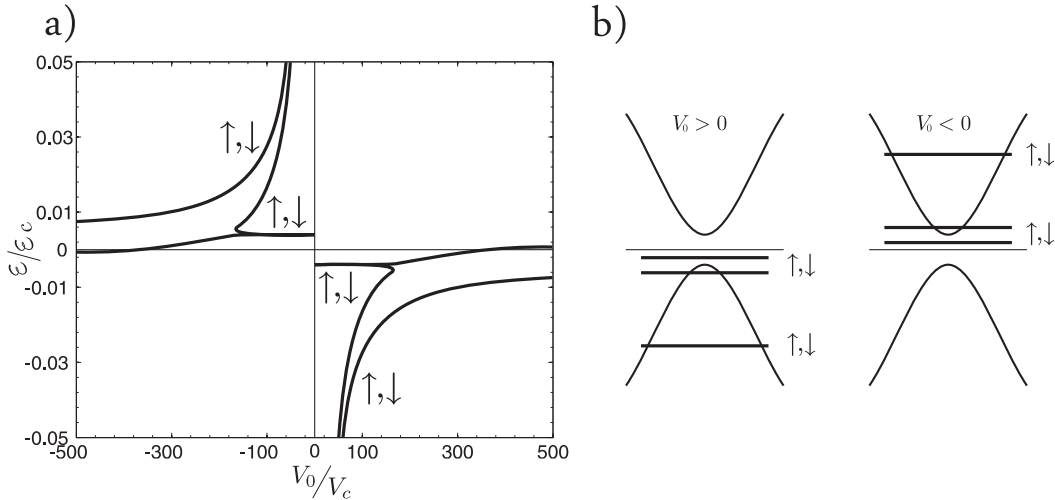


Figure 3. The location of impurity levels as a function the impurity strength parameter V_0 (a) and the schematic presentation of the impurity levels (b) in the case of non-magnetic impurity.

The numerical solutions of Equation (19) and Equation (21) describing the states related to the Dirac point K , as well as the corresponding solutions related to the Dirac point K' are presented in Figure 3,a. The schematic representation of the levels is presented in Figure 3,b. All the levels are spin degenerate due to the overlapping solutions of equations, related to the nonequivalent Dirac points. We used the parameters with much larger SO gap Δ to visualize better the character of solutions. If the state is located within the gap, the impurity level is discrete. For the level with energy $|\varepsilon_\uparrow| > \Delta$, it is a resonant state of width $\text{Im} F_\uparrow(\varepsilon_\uparrow)$. It should be noted that

$\text{Im} F_{\uparrow}(\varepsilon)$ is not the density of states in graphene because Equation (9) does not include the trace over sublattices.

It should be noted that both impurity states with energies ε_{\uparrow} and ε_{\downarrow} are mostly localized at the site of A sublattice in accordance with the assumption that the impurity potential (3) is located on the A-site. However, the real spread of the wavefunction can be much larger than the distance between nearest A and B sites.

4. Magnetic impurity

In the case of magnetic impurity we choose perturbation, which is different in sign for the spin up and down electrons, $V_{\mathbf{k}\mathbf{k}'\downarrow} = -V_{\mathbf{k}\mathbf{k}'\uparrow}$, and $V_{\mathbf{k}\mathbf{k}'\uparrow}$ is described by Equation (5). The resulting impurity levels related to the Dirac points K and K' are to be found from the following equations

$$\varepsilon_{\uparrow,\downarrow}^K = \mp\Delta \mp \frac{4\pi v^2}{V_0 \ln \frac{v^2 k_m^2}{|\Delta^2 - \varepsilon_{\uparrow,\downarrow}^2}}. \quad (22)$$

$$\varepsilon_{\uparrow,\downarrow}^{K'} = \pm\Delta \mp \frac{4\pi v^2}{V_0 \ln \frac{v^2 k_m^2}{|\Delta^2 - \varepsilon_{\uparrow,\downarrow}^2}}. \quad (23)$$

There is the spin splitting of the states related to the K point, which does not vanish as $\Delta \rightarrow 0$, and the resulting magnetization of impurity states is not compensated by another point K' . Corresponding numerical solutions of equations (22) and (23) are presented in Figure 4.

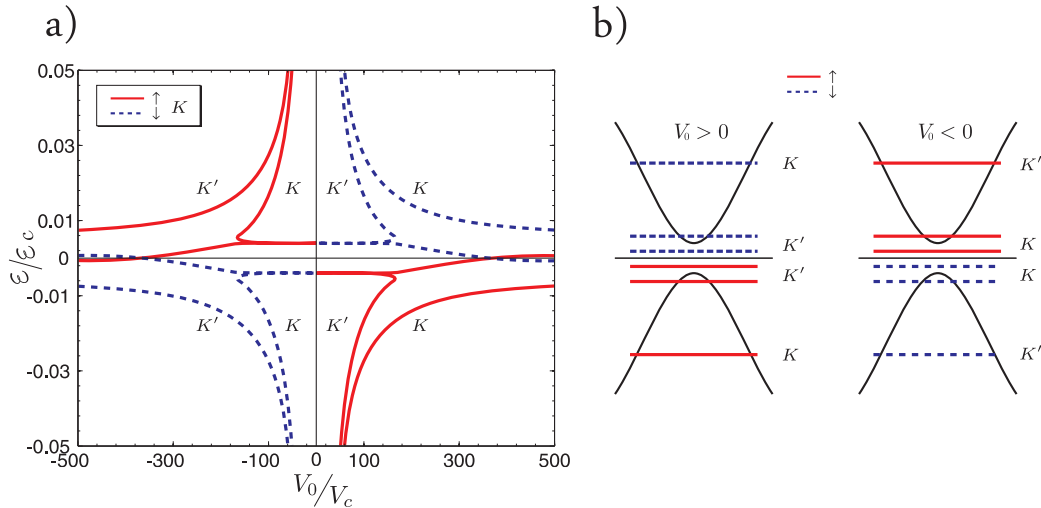


Figure 4. The same dependences as in Figure 3 in the case of magnetic impurity.

5. Nonmagnetic impurity with strong SO interaction

Using the same formalism, one can consider the impurity, which locally enhances the internal SO interaction. In this case the corresponding perturbation for K point has the form

$$\hat{V}_\Delta = \begin{pmatrix} \sigma_z \Delta_0 & 0 \\ 0 & 0 \end{pmatrix}, \quad (24)$$

where Δ_0 is the local After substitution of $V_0 \rightarrow \Delta_0$, the solution for the K point does not differ from the case of magnetic impurity considered above. However, for the point K' we have to change the sign of Δ_0 . As a result we obtain

$$\varepsilon_{\uparrow,\downarrow}^K = \mp \Delta \mp \frac{4\pi v^2}{\Delta_0 \ln \frac{v^2 k_m^2}{|\Delta^2 - \varepsilon_{\uparrow,\downarrow}^2|}}. \quad (25)$$

$$\varepsilon_{\uparrow,\downarrow}^{K'} = \pm \Delta \pm \frac{4\pi v^2}{\Delta_0 \ln \frac{v^2 k_m^2}{|\Delta^2 - \varepsilon_{\uparrow,\downarrow}^2|}}. \quad (26)$$

In this case the spin splitting of the states related to the point K does not vanish as $\Delta \rightarrow 0$ but the resulting local magnetization is absent due to the states from point K' . The solutions of equations (25) and (26) are presented in figure 5.

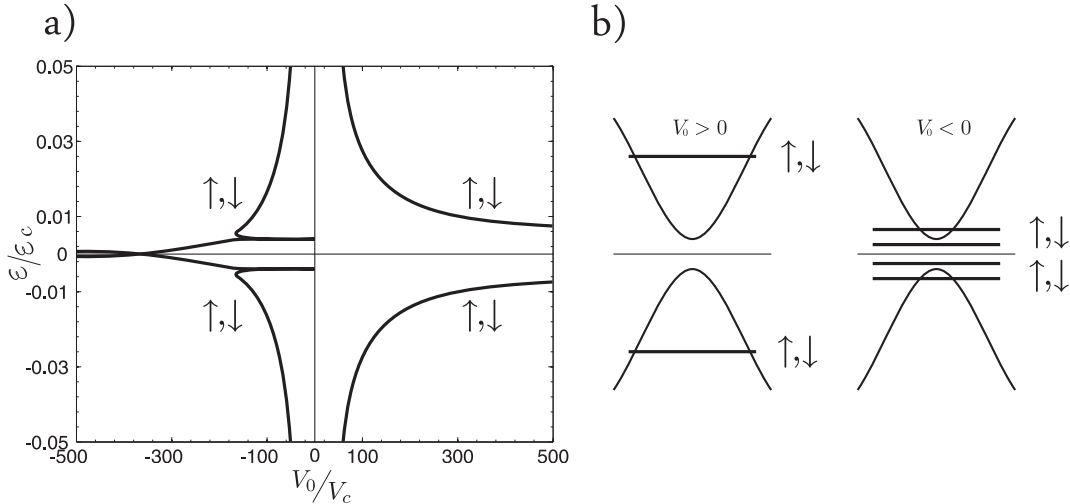


Figure 5. The same dependences as in Figure 3 in the case of spin-orbit impurity.

6. Wave function of the localized impurity state

Using the Schrödinger equation for the wave function, one can find the equation for impurity state [16]

$$\psi_i(\mathbf{r}) = \int d^2\mathbf{r}' \hat{G}(\mathbf{r}, \mathbf{r}'; \varepsilon) \hat{V}(\mathbf{r}') \psi_i(\mathbf{r}'), \quad (27)$$

where the Green function of free electrons in coordinate representation obeys

$$(\varepsilon - \hat{H}_{\mathbf{r}}) \hat{G}(\mathbf{r}, \mathbf{r}'; \varepsilon) = \delta(\mathbf{r} - \mathbf{r}'). \quad (28)$$

For the impurity located at $\mathbf{r} = 0$ we obtain from (27)

$$\psi_i(\mathbf{r}) = \hat{G}(\mathbf{r}, 0; \varepsilon) \hat{T}(\varepsilon) \psi_0(0), \quad (29)$$

where $\psi_0(\mathbf{r})$ is the eigenfunction of unperturbed Hamiltonian (1)

$$(\varepsilon - \hat{H}_{\mathbf{r}}) \psi_0(\mathbf{r}) = 0. \quad (30)$$

The Green function for Hamiltonian (3) has been calculated before [17]

$$\begin{aligned} \hat{G}_{\uparrow}(\mathbf{r}, \mathbf{r}'; \varepsilon) = & -\frac{i(\varepsilon - \Delta\tau_z)}{4v^2} H_0^{(1)} \left(\frac{|\mathbf{r} - \mathbf{r}'| \sqrt{\varepsilon^2 - \Delta^2}}{v} \right) \\ & + (\mathbf{r} - \mathbf{r}') \cdot \boldsymbol{\tau} \frac{\sqrt{\varepsilon^2 - \Delta^2}}{4v^2 |\mathbf{r} - \mathbf{r}'|} H_1^{(1)} \left(\frac{|\mathbf{r} - \mathbf{r}'| \sqrt{\varepsilon^2 - \Delta^2}}{v} \right). \end{aligned} \quad (31)$$

Thus, for the spin-up impurity state with energy ε_{\uparrow}

$$|\psi_{i\uparrow}(\mathbf{r})|^2 \sim \left| H_0^{(1)} \left(\frac{r \sqrt{\varepsilon_{\uparrow}^2 - \Delta^2}}{v} \right) \right|^2 + \left| H_1^{(1)} \left(\frac{r \sqrt{\varepsilon_{\uparrow}^2 - \Delta^2}}{v} \right) \right|^2 \sim e^{-2r/R_0}, \quad (32)$$

where $H_{\nu}^{(1)}(z)$ are the Hankel functions [18] and $R_{0\uparrow} = v/|\varepsilon_{\uparrow}^2 - \Delta^2|^{1/2}$ is the characteristic radius of the impurity wavefunction.

The function $\psi_0(\mathbf{r})$ in Equation (29) can be calculated using (30). Denoting the bispinor components $\psi_0^T(\mathbf{r}) = (\varphi^T(\mathbf{r}), \chi^T(\mathbf{r}))$ we find the relation

$$\chi(\mathbf{r}) = \frac{-iv(\partial_x + i\partial_y)}{\Delta + \varepsilon} \varphi(\mathbf{r}). \quad (33)$$

The equation for the function φ_{\uparrow} with the Hamiltonian (3) in polar coordinates (r, α) reads

$$\left(\frac{\partial^2}{\partial r^2} + \frac{1}{r} \frac{\partial}{\partial r} + \frac{1}{r^2} \frac{\partial^2}{\partial \alpha^2} - \kappa_{\uparrow}^2 \right) \varphi_{\uparrow}(r, \alpha) = 0, \quad (34)$$

which has the following solutions decaying at large r

$$\varphi_{\uparrow}(r, \alpha) = K_m(\kappa_{\uparrow} r) e^{im\alpha}, \quad (35)$$

where $\kappa_{\uparrow} = (\Delta^2 - \varepsilon_{\uparrow}^2)/v^2$, $K_m(z)$ is the modified Bessel function and $m \in Z$. Then the corresponding χ_{\uparrow} -component can be found from (33) and (35)

$$\chi_{\uparrow}(r, \alpha) = -\frac{iv\kappa_{\uparrow}}{\Delta + \varepsilon_{\uparrow}} K_{m+1}(\kappa_{\uparrow} r) e^{i(m+1)\alpha}. \quad (36)$$

Thus, up to the normalization we have

$$\psi_{0\uparrow m}(r, \alpha) = \begin{pmatrix} (\Delta + \varepsilon_{\uparrow}) K_m(\kappa_{\uparrow} r) e^{im\alpha} \\ -iv\kappa_{\uparrow} K_{m+1}(\kappa_{\uparrow} r) e^{i(m+1)\alpha} \end{pmatrix} \quad (37)$$

It should be noted that for $\psi_0(0)$ in Equation (29) we have to use the cutoff at small distance $r_c \sim k_{max}^{-1} \gg a_0/\pi$, where a_0 is the lattice constant and k_{max} is the upper limit for the Dirac model in graphene. It means that using the Dirac model we can find the impurity wave function at distances much larger than a_0 . On the other hand, as we see from (32), the radius of the impurity states R_0 near the Dirac point is much larger than this limit.

7. Conclusions

We have calculated the energies and wave functions of impurity states near the Dirac points in graphene taking into account the SO interaction. The calculations show the SO-induced spin splitting of these states. The existence of two nonequivalent Dirac points in the Brillouin zone leads to the spin degeneracy of the states with different spin. It should be noted that in principle the valley degeneracy can be broken by inhomogeneous deformations, which would result in the appearance of local magnetization.

Acknowledgments

This work was supported by the Polish Ministry of Science and Higher Education as a research project in years 2007 – 2010.

References

- [1] Novoselov K S, Geim A K, Morozov S V, Jiang D, Zhang Y, Dubonos S V, Grigorieva I V and Firsov A A 2004 *Science* **306** 666–669
- [2] Novoselov K S, Geim A K, Morozov S V, Jiang D, Katsnelson M I, Grigorieva I V, Dubonos S V and Firsov A A 2005 *Nature* **438** 197–200
- [3] Geim A K and Novoselov K S 2007 *Nat Mater* **6** 183–191
- [4] Katsnelson M I 2007 *Materials Today* **10** 20–27 ISSN 1369-7021
- [5] Schedin F, Geim A K, Morozov S V, Hill E W, Blake P, Katsnelson M I and Novoselov K S 2007 *Nat Mater* **6** 652–655
- [6] Castro Neto A H, Guinea F, Peres N M R, Novoselov K S and Geim A K 2009 *Rev. Mod. Phys.* **81** 109–162
- [7] Pereira V M, Guinea F, Lopes dos Santos J M B, Peres N M R and Castro Neto A H 2006 *Phys. Rev. Lett.* **96** 036801
- [8] Peres N M R, Guinea F and Castro Neto A H 2006 *Phys. Rev. B* **73** 125411
- [9] Hu B Y K, Hwang E H and Das Sarma S 2008 *Phys. Rev. B* **78** 165411
- [10] Pereira V M, Lopes dos Santos J M B and Castro Neto A H 2008 *Phys. Rev. B* **77** 115109
- [11] Kane C L and Mele E J 2005 *Phys. Rev. Lett.* **95** 226801
- [12] Min H, Hill J E, Sinitzyn N A, Sahu B R, Kleinman L and MacDonald A H 2006 *Phys. Rev. B* **74** 165310
- [13] Huertas-Hernando D, Guinea F and Brataas A 2006 *Phys. Rev. B* **74** 155426
- [14] Yao Y, Ye F, Qi X L, Zhang S C and Fang Z 2007 *Phys. Rev. B* **75** 041401
- [15] Gmitra M, Kunschuh S, Ertler C, Ambrosch-Draxl C and Fabian J 2009 *Phys. Rev. B* **80** 235431
- [16] Ziman J M 1969 *Elements of Advanced Quantum Theory* (Cambridge Univ. Press, Cambridge)
- [17] Dugaev V K, Litvinov V I and Barnas J 2006 *Phys. Rev. B* **74** 224438
- [18] Abramowitz M and Stegun I A 1964 *Handbook of Mathematical Functions* Natl. Bur. Stand. Appl. Math. Ser. 55 (National Bureau of Standards, Washington, DC, 1964)